Rapid Communication

Magnetic anisotropy and magnetization reversal of ultrathin iron films with in-plane magnetization on Si(111) substrates*

Liu Hao-Liang(刘郝亮), He Wei(何 为), Du Hai-Feng(杜海峰), Fang Ya-Peng(房亚鹏), Wu Qiong(吴 琼), Zhang Xiang-Qun(张向群), Yang Hai-Tao(杨海涛), and Cheng Zhao-Hua(成昭华)†

State Key Laboratory of Magnetism and Beijing National Laboratory for Condensed Matter Physics, Institute of Physics, Chinese Academy of Sciences, Beijing 100190, *China*

(Received 19 March 2012; revised manuscript received 9 April 2012)

The magnetic anisotropy and magnetization reversal of single crystal Fe films with thickness of 45 monolayer (ML) grown on Si(111) have been investigated by ferromagnetic resonance (FMR) and vibrating sample magnetometer (VSM). Owing to the significant modification of the energy surface in remanent state by slight misorientation from (111) plane and a uniaxial magnetic anisotropy, the azimuthal angular dependence of in-plane resonance field shows a six-fold symmetry with a weak uniaxial contribution, while the remanence of hysteresis loops displays a two-fold one. The competition between the first and second magnetocrystalline anisotropies may result in the switching of in-plane easy axis of the system. Combining the FMR and VSM measurements, the magnetization reversal mechanism has also been determined.

Keywords: magnetic anisotropy, magnetization reversal, ultrathin film

PACS: 75.30.Gw, 75.70.Ak, 68.55.–a **DOI:** 10.1088/1674-1056/21/7/077503

1. Introduction

The epitaxial ferromagnetic films on semiconductor substrates, a prototypical system for magnetoelectronics, and the integration of magnetic devices in semiconductor technology, have been widely studied for decades.[1] Especially, the Fe film on Si(111) substrate has attracted much attention owing to its some unique features,[2,3] which mainly lie in three aspects: first, the Si(111) substrate, due to its rich physics and the accurately controllable step width and type,[4−6] is often chosen as the step surface to tune the magnetic properties of ferromagnetic films;[7−9] second, a (111) oriented single crystal film seems to be more favorable than (100) or (110) oriented ones for magnetic softness,[10] since the former provides very low in-plane anisotropy; third, some interesting magnetic phenomena, such as four-fold symmetry of the in-plane ferromagnetic resonance (FMR) field and inverted hysteresis loops, have been observed due to the extreme sensitivity of magnetic properties to the small misorientation of Fe films from the (111) plane and the competitive magnetic anisotropies.[11,16] In order to deeply understand the magnetic properties of Fe(111) films, the accurate measurement of the magnetic anisotropies of Fe(111) films is necessary.

Analysis of the magnetic anisotropy of materials is typically carried out by using the ferromagnetic resonance (FMR) method. For Fe(111) films on Si(111) substrates, two alternative approaches are often adopted by either transverse biased initial inverse susceptibility and torque (TBIIST) or directly reproducing the in-plane hysteresis loops. However, the former one cannot measure the first-order cubic anisotropy, and the magnetization reversal model must first be assumed in the latter. Compared with magnetization curve fitting, the FMR technique yields precise results, but is irrelative to the magnetization reversal mechanisms. If we combine the two methods together, both the magnetic anisotropy and magne-

*Project supported by the National Basic Research Program of China (Grant Nos. 2009CB929201, 2010CB934202, and 2011CB921801) and the National Natural Science Foundation of China (Grant Nos. 50931006, 11034004, and 51021061).

†Corresponding author. E-mail: zhcheng@iphy.ac.cn

© 2012 Chinese Physical Society and IOP Publishing Ltd

tization reversal can be determined. In addition, it is well known that the magnetocrystalline anisotropy energy in the (111) plane exhibits six-fold symmetry only related to the weak second-order cubic anisotropy constant K_2. Hence, the first-order cubic anisotropy constant K_1 is often neglected in analyzing the experimental results.

In the present paper, we have investigated the magnetic anisotropy and magnetization reversal of molecular beam epitaxy (MBE)–grown 45-monolayer (ML) Fe/p(2×2) iron silicide/Si(111) by the FMR and vibrating sample magnetometer (VSM) methods. A nominal flat Si(111) substrate (with a miscut angle of only 0.1° along the [11–2] direction) is chosen for weakening the effect of misorientation from the (111) plane. The remanence of the system shows an in-plane two-fold symmetry. However, a six-fold one of the in-plane resonance field is visible. The energy surface of Fe(111) in a remnant state has been significantly modified by the very slight misorientation from the (111) plane and the in-plane uniaxial magnetic anisotropy. Meanwhile, the competition between two cubic terms K_1 and K_2 may result in the switching of the direction of the in-plane easy axis. Combining the fitting magnetic parameters and magnetic hysteresis loops, the magnetization reversal mechanism is also determined.

2. Experiments

The growth experiments were performed in an ultrahigh vacuum (UHV) molecular beam epitaxy chamber with the base pressure of 2×10^{-10} mbar. The UHV chamber is equipped with a scanning tunneling microscope (STM) and a low-energy electron diffraction (LEED) system. Substrates were Si(111) wafers with a miscut angle $\beta = 0.1°$ along the [11–2] direction. An atomically clean 7×7 Si(111) surface of the sample was obtained after a well-established flashing procedure. The Fe film with a thickness of 45 ML was deposited in a two-step process.[10] First, a well ordered 2×2 reconstructed iron silicide seed layer constructed by depositing 1.5-ML Fe annealed to 700 K for 10 min, was inserted between the substrates and Fe films in order to prevent the Fe/Si intermixing.[11] Subsequently, Fe was deposited on the iron silicide template at room temperature, with the normal incidence direction being perpendicular to the substrate plane at a deposition rate of 1.5 ML/min. The atomic density of 1 ML corresponds to 7.8×10^{14} cm^{-2}, which is the same as the unreconstructed Si(111) surface. STM, FMR, and VSM measurements were performed at room temperature. A coordinate system used in experimental measurements is defined by the polar angle θ and azimuthal angle φ with respect to the film normal and step direction in the sample plane, respectively. NaCl with a thickness of 14 ML was deposited on the sample as a capping layer to protect samples from being oxidized.[10]

3. Results and discussion

Figure 1(a) shows a large-scale STM image of a p(2 × 2) reconstructed iron silicide seed layer (evidenced by the LEED pattern in the left–upper inset of Figure 1(a)), which well reproduces the bare Si(111) structure of double-layer high (0.31 nm) step arrays with the average terrace width of 160 nm corresponding closely to the nominal miscut of 0.1°. The atomic resolution STM image including the island and terrace, as shown in the right–bottom inset of Fig. 1(a), indicates that they are composed of the same p(2 × 2) reconstructed silicide structure.[12] A three-dimensional (3D) grown inhomogeneous-shaped *bcc*–Fe(111) film with azimuth orientations Fe(111)||Si(111) and Fe[–1–12]||Si[11–2][2] is displayed in Fig. 1(b). The surface morphology of Fe films consists of small grains (10–25 nm) and completely covers the iron silicide buffer layer.

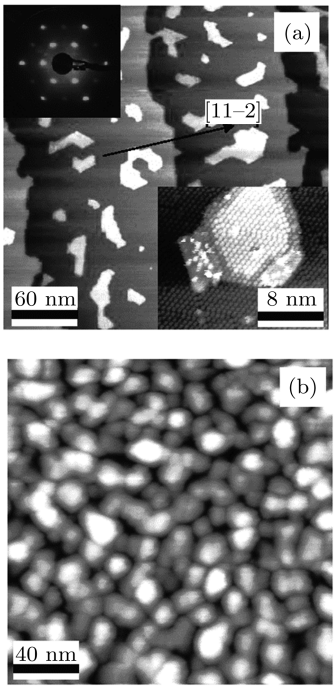


Fig. 1. (a) STM image of the p(2 × 2) iron silicide buffer layer. Left–top: LEED pattern taken at the primary electron energy of 28 eV, right–bottom: atomic resolution image of the iron silicide. (b) STM image of the inhomogeneous-shaped *bcc*-Fe(111) film with a thickness of 45 ML.

The magnetic anisotropies of the sample were measured by FMR at a frequency of 9.0 GHz. An external field H is applied to the film plane in different directions. The azimuthal angle φ dependence of the FMR spectra and resonance field $H_{\rm r}$ are displayed in Figs. 2(a) and 2(b), respectively. The $H_{\rm r}(\varphi)$ curve presents two contributions of both a strong cubic six-fold symmetry and a weak two-fold one. It indicates that the in-plane magnetic anisotropy is the superposition of a dominant six-fold and a small uniaxial magnetic anisotropy contribution, which is in good agreement with the crystalline structures of the nominal flat Si(111) plane and single crystal Fe(111) film. In order to analyze the experimental data, the total free energy density of the system is written in the following form:[11,13]

$$\begin{aligned} E = & -\mu_0 M_{\rm s} H\cdot\boldsymbol{\mu} + K_1\alpha_1^2\alpha_2^2 + \alpha_2^2\alpha_3^2 + \alpha_3^2\alpha_1^2 \\ & + K_2(\alpha_1^2\alpha_2^2\alpha_3^2) - K_{\rm u}(\boldsymbol{\mu}\cdot\boldsymbol{n}_{\rm u})^2 + K_{\rm d}(\boldsymbol{\mu}\cdot\boldsymbol{n}_{\rm d})^2 \\ & - K_s(\boldsymbol{\mu}\cdot\boldsymbol{n}_s)^2. \end{aligned} \quad (1)$$

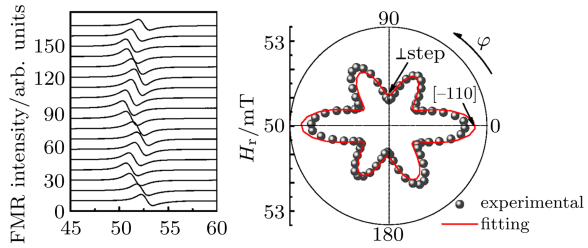


Fig. 2. (colour online) (a) Experimental FMR spectra. (b) Experimental and fitted data of resonance field $H_{\rm r}(\varphi)$. The $\varphi = 0$ direction is in line with the step direction [–110].

The first three terms are, respectively, the Zeeman energy, the first- and second-order cubic magnetocrystalline anisotropy energies, with $\boldsymbol{\mu}$ being the unit vector of the magnetization vector, $M_{\rm s}$ being the saturation magnetization of Fe (taken to be the bulk value of 1.74×10^6 A/m), and α_i being the directional cosines of the magnetization vector with respect to cubic axes [100], [010], and [001]. The last three terms refer to the in-plane uniaxial magnetic anisotropy with its easy axis along the step direction $\boldsymbol{n}_{\rm u}(\theta = 90^\circ, \varphi = 0^\circ)$, the out-of-plane demagnetization energy with its hard axis $\boldsymbol{n}_{\rm d}$ normal to the small vicinal plane rather than the (111) crystallographic plane, and the surface magnetic anisotropy with its easy axis $\boldsymbol{n}_s$ normal to the (111) plane. The $K_{\rm u}$, $K_{\rm d}$, and $K_{\rm s}$ are constants, and $K_{\rm d} = \mu_0 M_{\rm s}^2$. Fitting the experimental data by using Eq. (1) and standard FMR conditions, we obtain the following results: $K_1 = 4.4\times10^4$ J/m^3, $K_2/K_1 = 0.05$, $K_{\rm s}/K_{\rm d} = 0.184$, and $K_{\rm u} = -5.9\times10^2$ J/m^3. The negative value of the in-plane uniaxial magnetic anisotropy constant $K_{\rm u}$ indicates that the direction of easy axis is perpendicular to the step direction. Similar phenomena have been reported in the system Fe/W(001)[14] or Au/Co/Cu/Si(111),[15] which have been explained by the step-induced anisotropy. Garreau *et al.* reported the uniaxial anisotropy in the Fe(111)/c(8×4) iron silicide/Si(111) system with random directions of the easy axis at different Fe thicknesses.[2] They excluded the origin of uniaxial anisotropy from symmetry breaking since the distinct samples with the same nominal thickness present different uniaxial directions. Here, the samples with different nominal thicknesses present the same uniaxial directions. Hence, the uniaxial anisotropy may result from the symmetry breaking due to the small vicinality (0.1°) of the nominal (111) surface.

The FMR equation of a Fe-(111) surface including K_1 and K_2 terms has been derived by Kohmoto[16] using an approximate method of effective demagnetizing factors, in which the in-plane six-fold oscillation of resonance field $H_{\rm r}$ only originates from the K_2 term. No angular variation of $H_{\rm r}$ is expected by K_1 term. However, accurate numerical calculation can make sure that the six-fold symmetry of in-plane resonance field $H_{\rm r}$ and reduced anisotropy energy $E_{\rm r}$ may be observed even when $K_2 = 0$, as shown in Fig. 3(a). This can be explained by considering the competition between the K_1 term and effective demagnetizing field term$\big(K_{\rm d} - K_s\big)$, resulting in a small deviation of magnetization with respect to the Fe(111) plane in the resonance condition. Furthermore, as can be seen in Fig. 3, when $(K_2 = 0)$, the easy axes of the system with positive K_1 are along six equivalent $\langle11-2\rangle$ directions (one of them is perpendicular to the step direction). According to the expression of the second cubic energy term in the (111) film $E_2^{(111)} = K_2(1+\cos6\varphi)/108$,[2] a positive value of K_2 relates to the easy axis along six equivalent $\langle-110\rangle$ directions (one of them is parallel to the step direction), as displayed in Fig. 3 $(K_1 = 0)$. Though the value of K_1 is generally one order larger than that of K_2, they have a comparable influence on the in-plane resonance field. The competitive effects of K_1 and K_2 terms on $H_{\rm r}$ may be clearly displayed by defining a parameter $\Delta H_{\rm r} = H_{\rm r}^0 - H_{\rm r}^{90}$ (the difference of the resonance field between the azimuthal angle $\varphi = 0^\circ$ and $\varphi = 90^\circ$, i.e., parallel and perpendicular to the step

direction, respectively). If $\Delta H_r > 0$, the easy axis is along $\langle 11-2\rangle$ directions. Otherwise, if $\Delta H_r < 0$ the easy axis is along $\langle -110\rangle$ directions. The ΔH_r dependence of K_1 and K_2 (with $K_s/K_d = 0.184$, $K_u = 0$, and $\beta = 0$) is illustrated in Fig. 3(b). The whole region is divided into two parts with different easy axes by the thick solid lines of $\Delta H_r = 0$. The six-fold anisotropy easy axis switches from $\langle -110\rangle$ in area i to $\langle 11-2\rangle$ in area ii is displayed.

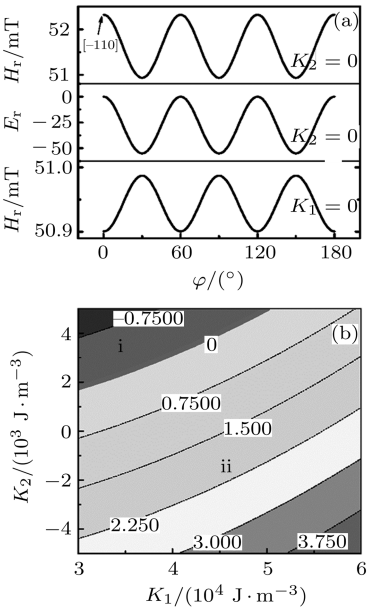


Fig. 3. (a) In-plane angular dependence of the anisotropy energy and resonance field; (b) difference ΔH_r between the parallel resonance field H_r^0 and perpendicular resonance field H_r^{90} to the step direction as a function of K_1 and K_2. $K_s/K_d = 0.184$, $K_u = 0$, and $\beta = 0.0$.

To further investigate the magnetization reversal behavior, the magnetic properties of the samples are also measured by using the VSM method. Figure 4 shows four representative hysteresis loops for $\varphi = 0°, 15°, 30°$, and $75°$ (denoted by hollow diamonds), indicating that the system is the supposition of in-plane uniaxial anisotropy and cubic anisotropies. The loops with low remanence correspond to $\boldsymbol{H}$ parallel to the step direction, while the almost rectangular loops represent $\boldsymbol{H}$ perpendicular to the step direction, indicating the direction of easy axis of in-plane uniaxial magnetic anisotropy is perpendicular to the step direction, which is consistent with the FMR measurements.

By using the fitting magnetic parameters and the coherent rotation model, the calculated magnetization curves are obtained by minimizing the free energy of the system, as shown by the solid lines in Fig. 4. For the field close to the hard axis, there is an excellent agreement between experimental and calculated data. A split loop for $\varphi = 0°$ is observed and characterized by a shift field H_s with the value $H_s = K_u/\mu_0 M_s$.[17] A deviation of 5° from the exact hard axis is considered as the experimental error in the fitting. The in-plane uniaxial magnetic anisotropy constant can also be obtained as $K_u \approx 5.2 \times 10^2$ J/m^3, showing a good agreement with the FMR measurements. While in the vicinity region of the easy axis, the calculated coercivity is much larger than the experimental one. In this case, the magnetization reversal mechanism deviates from the coherent rotation.

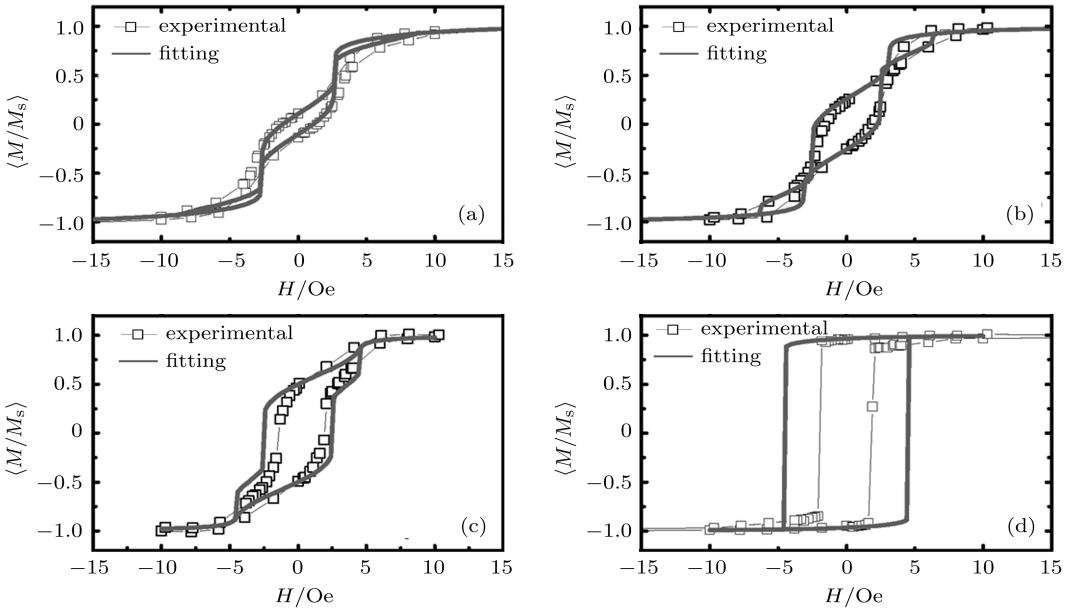


Fig. 4. In-plane hysteresis loops for representative magnetic field angles of (a) 0°, (b) 15°, (c) 30°, and (d) 75°.

The comparison of the remanence and coercivity in the whole azimuthal angular range between the experimental and simulated data is plotted in Fig. 5. Despite the big deviation of $H_c(\varphi)$ curves, the $M_R/M_s(\varphi)$ curves show a good consistency and can be well fitted by using a simple equation $|\sin(\varphi)|$. Santos *et al.* presented a similar two-fold symmetry of the $M_R/M_s(\varphi)$ curve in the Fe(6 nm)/Si(111) system, but didn't explain it.[8] In addition, the six-fold symmetry of the experimental $H_c(\varphi)$ curve is visible in this system. However, in the current sample, both $M_R/M_s(\varphi)$ and $H_c(\varphi)$ curves don't reveal six-fold symmetry of the in-plane cubic magnetic anisotropy. For a nominal flat Fe(111) film, the cubic Fe anisotropy overwhelms the uniaxial one, the six-fold symmetry should be revealed both in azimuthal angular dependence of resonance field and remanence. In order to clarify the reason behind the anomalous behavior of azimuthal angular dependence of resonance field and remanence in our experiment, a more in-depth understanding of the origins of remanence and coercivity is required.

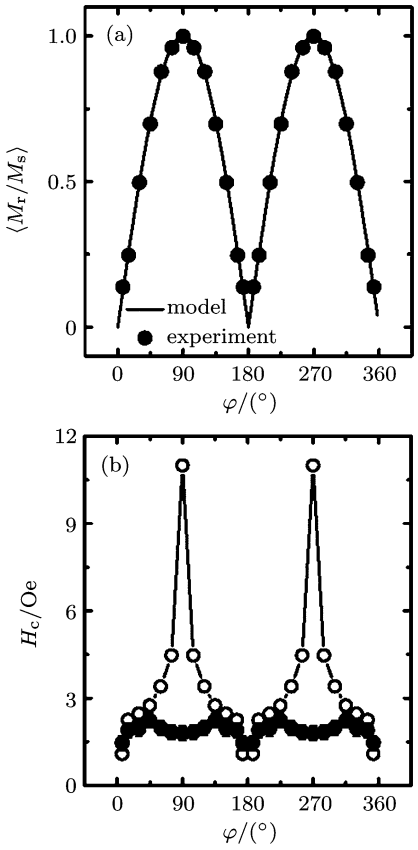


Fig. 5. Azimuthal dependence of the experimental and calculated (a) remanence and (b) coercivity.

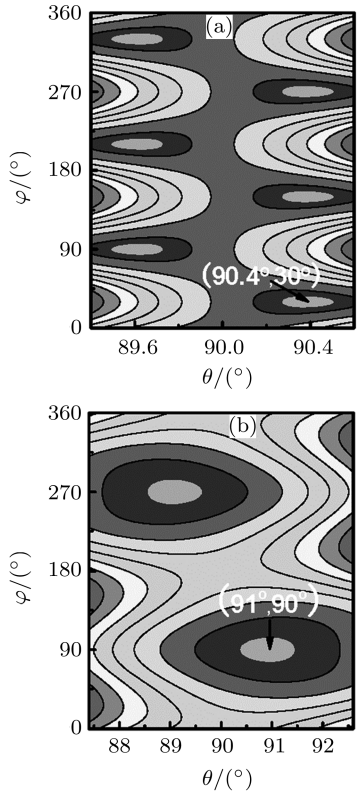


Fig. 6. Reduced energy surface with (a) $K_u = 0$ and $\beta = 0$, six minima are seen; (b) $K_u \approx 5.2 \times 10^2$ J/m^3 and $\beta = 0.1^o$, only two minima are observed.

Remanence is defined as the magnetization value in a system after an external magnetic field is removed. Neglecting the thermal activated energy and under the assumption of single domain state, the magnetic moments of the system in remanent state would point to the directions corresponding to the minima in the energy surface in zero field. Thus, we plot the energy surface of the Fe(111) film in the vicinity of the Si(111) plane at zero field with different parameters in Figs. 6(a) and 6(b), respectively. In the case of $\beta = 0$ and $K_u = 0$, i.e., a perfect crystalline Fe(111) film without the uniaxial anisotropy, the six energy minima displayed by light gray ellipses in Fig. 6(a), is revealed by the energy contour. The direction of magnetization of the system in a remanent state would only correspond to one of them. The remanence is deduced to be the cosine of the angle between magnetic field direction and the nearest minima for the magnetization. Consequently, a six-fold symmetry of in-plane remanence is predicted. Considering the effect of the small miscut angle $\beta = 0.1^\circ$ and the in-plane uniaxial magnetic anisotropy $K_u \approx 5.2 \times 10^2$ J/m^3, the energy contour is significantly modified, as shown in Fig. 6(b). Only two minima are left. Thus, a two-fold symmetry

of in-plane remanence is displayed, which is consistent with the experimental observations. The coercivities depend on both the total energy of system and the magnetization reversal mechanism. Thus, the six-fold symmetry of $H_c(\varphi)$ may not be always observed even in the case of predominant cubic anisotropy in the (111) plane. It depends on the effect of the vicinal plane and the uniaxial anisotropy on the magnetization reversal mechanism. In fact, the six-fold $H_c(\varphi)$ curves are seldom observed in Fe(111) films since a small vicinal angle or weak uniaxial anisotropy is usually sufficient to modify the energy surface of the system from six-order symmetry to two-fold one.

4. Conclusion

We have investigated the magnetic anisotropy and magnetization reversal of 45-ML Fe single crystal film on Si(111) substrates by using flat ultrathin p(2×2) iron silicide as a buffer layer. Due to the significant modification of the energy surface of the system by the very slight misorientation from the (111) plane and uniaxial magnetic anisotropy, a two-fold remanence of the system is displayed, while the six-fold symmetry of the in-plane resonance field is still visible. Meanwhile, the competition between first and second magnetocrystalline anisotropy may result in the switching of the in-plane easy axis. The magnetization reversal mechanism is dominated by coherent rotation for the field close to the hard axis , and changes into domain wall motion around the easy axis.

References

[1] Zutic I, Fabian J and Sarma S D 2004 *Rev. Mod. Phys.* **76** 323

[2] Garreau G, Hajjar S, Bubendorff J L, Pirri C, Berling D, Mehdaoui A, Stephan R, Wetzel P, Zabrocki S, Gewin G, Boukari S and Beaurepaire E 2005 *Phys. Rev.* B **71** 094430

[3] Kataoka K, Hattori K, Miyatake Y and Daimon H 2006 *Phys. Rev.* B **74** 155406

[4] Men F K, Liu F, Wang P J, Chen C H, Cheng D L, Lin J L and Himpsel F J 2002 *Phys. Rev. Lett.* **88** 096105

[5] Stupakiewicz A, Vedmedenko E Y, Fleurence A, Maroutian T, Beauvillain P, Maziewski A and Wiesendanger R 2009 *Phys. Rev. Lett.* **103** 137202

[6] Endo Y, Okamoto S, Kitakami O and Shimada Y 1996 *J. Appl. Phys.* **81** 344

[7] Rezende S M, Moura J A S and Aguiar F M 1994 *Phys. Rev.* B **49** 15105

[8] Santo M C, Geshev J, Schmidt J E, Teixeira S R and Pereira L G 1994 *Phys. Rev.* B **61** 1311

[9] Kak M, Stephan R, Mehdaoui A, Berling D, Bolmont D, Gewinner G and Wetzel P 2004 *Surf. Sci.* **566** 278

[10] Sun D L, Wang D Y, Du H F, Ning W, Gao J H, Fang Y P, Zhang X Q, Sun Y, Cheng Z H and Shen J 2009 *Appl. Phys. Lett.* **94** 012504

[11] Du H F, He W, Liu H L, Fang Y P, Wu Q, Zou T, Zhang X Q, Sun Y and Cheng Z H 2010 *Appl. Phys. Lett.* **96** 142511

[12] Hajjar S, Garreau G, Pelletier S, Bolmont D and Pirri C 2003 *Phys. Rev.* B **63** 033302

[13] Stupakiewicz A, Maziewski A, Matlak K, Spiridis N, Ślęak M, Ślęakak T, Zaja M and Korecki 2008 *Phys. Rev. Lett.* **101** 217202

[14] Chen J and Erskine J L 1992 *Phys. Rev. Lett.* **68** 1212

[15] Stupakiewicz A, Kirilyuk A, Fleurence A, Gieniusz R, Maroutian T, Beauvillain P, Maziewski A and Rasing Th 2009 *Phys. Rev.* B **80** 094423

[16] Kohmoto O 2004 *Jpn. J. Appl. Phys.* **43** 1334

[17] Bisio F, Moroni R, Mongeot F B, Canepa M and Mattera L 2006 *Phys. Rev. Lett.* **96** 057204